Determination of ϕ and χ_1 Angles in Proteins from $^{13}C-^{13}C$ Three-Bond *J* Couplings Measured by Three-Dimensional Heteronuclear NMR. How Planar Is the Peptide Bond?

Jin-Shan Hu and Ad Bax*

Contribution from the Laboratory of Chemical Physics, National Institute of Diabetes and Digestive and Kidney Diseases, National Institutes of Health, Bethesda, Maryland 20892-0520

Received January 8, 1997[⊗]

Abstract: A new pulse scheme, HN(CO)C, is described for simultaneous measurement of three-bond $^3J_{C'C^\beta}$ and $^3J_{C'C^\gamma}$ couplings in proteins uniformly enriched with ^{13}C and ^{15}N. The experiment is demonstrated for human ubiquitin and apo-calmodulin, which have rotational correlation times of 4 and 8 ns, respectively. A Karplus relation, $^3J_{C'C^\beta} = 1.59\cos^2(\phi - 120°) - 0.67\cos(\phi - 120°) + 0.27$ Hz, is obtained by correlating the ubiquitin $^3J_{C'C^\beta}$ values with backbone ϕ angles from its crystal structure. Using these crystal structure ϕ angles, the root-mean-square difference (rmsd) between experimental $^3J_{C'C^\beta}$ values and those predicted from the Karplus relation is 0.24 Hz. When using ϕ angles derived from $^3J_{HNH^\alpha}$, $^3J_{HNC^\beta}$, $^3J_{HNC'}$, $^3J_{H^\alpha C'}$, and $^3J_{C'C'}$, this rmsd decreases to 0.17 Hz. Peptide backbone ϕ angles can be derived from *J* couplings between either C'_{i-1} or H^N_i and the three C^α_i substituents, C'_i, C^β_i, H^α_i. For 45 residues in ubiquitin all six couplings have been measured, and the ϕ angles derived for these residues from couplings involving H^N_i agree to within experimental error (rmsd = 7.7°) with ϕ angles derived from the three *J* couplings to C'_{i-1}. This confirms that, on average, the angle between the $C'_{i-1}-N_i-C^\alpha_i$ and $H^N_i-N_i-C^\alpha_i$ planes is considerably less than 7.7° and excludes the possibility of large deviations from peptide bond planarity in α-helices. Intraresidue $^3J_{C'C^\gamma}$ couplings for aliphatic residues are found to range from 0.7 Hz for a *gauche* conformation to *ca.* 4 Hz for a *trans* conformation.

Three-bond $^{13}C-^{13}C$ *J* couplings show a Karplus-type[1] dependence on the intervening dihedral angle, and they have long been recognized as a valuable source of structural information.[2−4] For ^{13}C-enriched proteins, measurements have been primarily restricted to $^3J_{CC}$ couplings involving at least one methyl group, which, owing to its three degenerate protons and its rapid rotation about the 3-fold symmetry axis, yields superior sensitivity and resolution in ^1H-detected experiments. Such $^3J_{CC}$ couplings have been measured both by an E.COSY-type technique[5] and by quantitative *J* correlation methods.[6−8]

Recently, we described a new quantitative *J*-correlation experiment for measuring $^3J_{C'C'}$ between carbonyl and carbonyl/carboxyl carbons.[9] This experiment takes advantage of the relatively narrow line width of the unprotonated carbonyl resonances to measure these small $^{13}C'-^{13}C'$ *J* couplings. Here, we extend this approach to the simultaneous measurement of three-bond $^{13}C'$-^{13}C *J* couplings between the backbone carbonyl and aliphatic $^{13}C^\beta$ and $^{13}C^\gamma$ carbons. The experimental scheme, which we refer to as HN(CO)C, is again of the quantitative *J*-correlation type. In this scheme, magnetization is transferred from H^N, via its preceding carbonyl carbon, to aliphatic carbons that have a long-range *J* coupling to the carbonyl, followed by the reverse pathway and H^N detection.

$^3J_{C'C^\beta}$ and $^3J_{C'C^\gamma}$ values measured in human ubiquitin (76 residues), in combination with the corresponding intervening ϕ and χ_1 angles taken from the ubiquitin crystal structure,[10] are used to derive the first empirical Karplus curve parametrizations for these two types of *J* couplings. Measurement of $^3J_{C'C^\beta}$ and $^3J_{C'C^\gamma}$ is applicable to typical medium-sized proteins and is demonstrated for a sample of apo-calmodulin (148 residues) for which a rotational correlation time of ∼8 ns has been reported.[11]

The intraresidue $^3J_{C'C^\gamma}$ coupling is related to the side chain χ_1 angle and permits evaluation of this torsion angle, independent of the frequently poorly resolved proton resonances. The coupling is largest in the common situation where C^γ is oriented *trans* with respect to C′ (corresponding to $\chi_1 = -60°$ for most residue types). Correlations resulting from the $^3J_{C'C^\gamma}$ coupling are therefore commonly observed with our new experimental scheme and provide useful structural constraints, in addition to validation of $^{13}C^\gamma$ assignments. When $^3J_{C'C^\gamma}$ falls below the threshold needed to yield an observable cross-peak, this information frequently can be used to exclude a *trans* coupling, thus also constraining the χ_1 angle.

For most residues in ubiquitin, five different types of *J* couplings defining the polypeptide backbone angle ϕ have been reported previously.[9,12] The values of four of these, namely,

* To whom correspondence should be addressed. FAX: (301) 402-0907. Phone: (301) 496-2848. E-mail: bax@nih.gov.

[⊗] Abstract published in *Advance ACS Abstracts,* June 15, 1997.

(1) Karplus, M. *J. Chem. Phys.* **1959**, *30*, 11−15.
(2) Bystrov, V. F. *Prog. Nucl. Magn. Reson. Spectrosc.* **1976**, *10*, 41−81.
(3) Marshall, J. L. *Carbon-Carbon and Carbon-Proton NMR Couplings: Applications to Organic Stereochemistry and Conformational Analysis*; VCH: Deerfield Beach, FL, 1983.
(4) Krivdin, L. B.; Della, E. W. *Prog. Nucl. Magn. Reson. Spectrosc.* **1991**, *23*, 301−610.
(5) Schwalbe, H.; Rexroth, A.; Eggenberger, T.; Geppert, T.; Griesinger, C. *J. Am. Chem. Soc.* **1993**, *115*, 7878−7879.
(6) Bax, A.; Max, D.; Zax, D. *J. Am. Chem. Soc.* **1992**, *114*, 6923−6925.
(7) Bax, A.; Vuister, G. W.; Grzesiek, S.; Delaglio, F.; Wang, A. C.; Tschudin, R.; Zhu, G. *Methods Enzymol.* **1994**, *239*, 79−105.
(8) Grzesiek, S.; Vuister, G. W.; Bax, A. *J. Biomol. NMR* **1993**, *3*, 487−493.
(9) Hu, J.-S.; Bax, A. *J. Am. Chem. Soc.* **1996**, *118*, 8170−8171.
(10) Vijay-Kumar, S.; Bugg, C. E.; Cook, W. J. *J. Mol. Biol.* **1987**, *194*, 531−544.
(11) Tjandra, N.; Kuboniwa, H.; Ren, H.; Bax, A. *Eur. J. Biochem.* **1995**, *230*, 1014−1024.
(12) Wang, A. C.; Bax, A. *J. Am. Chem. Soc.* **1996**, *118*, 2483−2494. All rmsd values reported in this paper erroneously correspond to the mean absolute difference and therefore are between 10 and 20% smaller than the true rmsd values; this error does not have any noticeable effect on any of the reported Karplus parameters or other conclusions.

S0002-7863(97)00067-X

$^3J_{HNH^\alpha}$, $^3J_{HNC^\beta}$, $^3J_{HNC'}$, and $^3J_{C'H^\alpha}$, were found to be in excellent agreement with one another and suggested only small differences between the ϕ angles determined from these J couplings relative to the angles in the crystal structure.[12] However, it is important to note that $^3J_{HNH^\alpha}$, $^3J_{HNC^\beta}$, and $^3J_{HNC'}$ relate to the dihedral angle involving H^N, and not directly to ϕ itself; i.e., deriving ϕ from these couplings implicitly assumes the peptide bond to be planar.

The amide protons in ubiquitin were not observed in its X-ray structure, and in our previous NMR study[12] these hydrogens were added with the program XPLOR,[13] assuming planar peptide bonds. However, *ab initio* calculations for the geometry of unsolvated dipeptide analogs in vacuum suggest that the H−N bond vector generally makes a significant angle of *ca* 15° with the plane defined by C'_{i-1}, N_i, and C^α_i, both in α-helices and β-sheets.[14,15] A recent report by Sulzbach et al.[16] indicates that the C′ chemical shifts calculated for α-helices agree with experimental shifts only if significant pyramidalization of the amide moiety is introduced, whereas β-sheet amides do not require a distortion from planarity. Such deviations from planarity would make $^3J_{HNH^\alpha}$, $^3J_{HNC^\beta}$, and $^3J_{HNC'}$ poor reporters for the backbone angle ϕ.

In addition to $^3J_{C'H^\alpha}$ we now also have data for $^3J_{C'C^\beta}$ and $^3J_{C'C'}$, making it possible to determine the difference between dihedral angles involving H^α, C^β, and C′ atoms of residue i and either H^N_i or C'_{i-1}. For planar peptide bonds, ϕ angles derived from J couplings to C'_{i-1} are expected to be identical to those determined from J couplings to H^N_i. Thus, for the first time, we now can evaluate the planarity of peptide bonds independent of crystallographic information. For 45 residues in ubiquitin a complete set of six J couplings has been measured, and in this paper we report that the rmsd in ϕ angles derived from the three couplings to H^N_i and the corresponding couplings to C'_{i-1} equals 7.7°. This rmsd is comparable to the experimental uncertainty in the difference between the two sets of angles, and our data therefore indicate that the rms angle between the H^N_i−N_i−C^α_i and C'_{i-1}−N_i−C^α_i planes is considerably less than 7°, both in α-helical and β-strand backbone conformations.

Experimental Section

Uniformly $^{13}C/^{15}N$-enriched *Xenopus* calmodulin was obtained from overexpression in *Escherichia coli*, grown in M9 minimal medium, using [$^{13}C_6$]glucose and $^{15}NH_4Cl$. The NMR sample contained 10 mg of protein in 450 μL of solvent (1.3 mM), consisting of 5% D_2O/95% H_2O, 100 mM KCl, and 1.5 mM EDTA, pH 6.3.

$^{13}C/^{15}N$-enriched human ubiquitin was obtained commercially (VLI Research, Southeastern, PA) and used without further purification. A total of 3.5 mg of protein was dissolved in 220 μL of 5% D_2O/95% H_2O (1.8 mM) containing 30 mM sodium acetate buffer, pH 4.7. A Shigemi microcell (Shigemi Inc., Allison Park, PA) was used.

NMR spectra were recorded on Bruker AMX-600 and DMX-500 spectrometers, each equipped with a triple-resonance probehead containing a self-shielded z-gradient coil. Spectra for apo-calmodulin (apoCaM) were recorded at 23 °C, and for ubiquitin at 30 °C. The 3D HN(CO)C spectrum for human ubiquitin was recorded at 600 MHz as a 39* × 80* × 512* (n* refers to n complex data points) data matrix with acquisition times of 28.1 (t_1, ^{15}N), 8.0 (t_2, ^{13}C), and 56.3 ms (t_3, $^1H^N$). The total measuring time was 73 h. A 2D reference spectrum (39* × 512*) was recorded using the same pulse scheme but an alternate phase cycling scheme, as indicated in the legend to Figure 1.

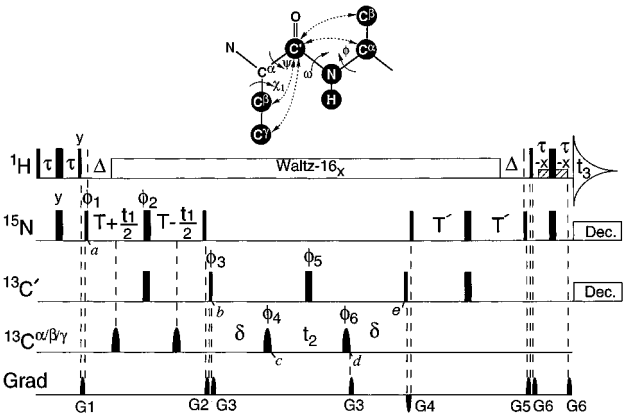

Figure 1. Pulse scheme for the 3D HN(CO)C experiment. Narrow and wide pulses denote 90° and 180° flip angles (except for shaded low power 90°$_{-x}$ ^1H pulses), respectively, and unless indicated the phase is x. Phase cycling: $\phi_1 = x$; $\phi_2 = 4(x), 4(y), 4(-x), 4(-y)$; $\phi_3 = x$; $\phi_4 = x, -x$; $\phi_5 = 8(x), 8(y)$; $\phi_6 = 2(x), 2(-x)$; receiver = P, $2(-P)$, P, where $P = x, -x, -x, x$. For acquisition of the 2D reference spectrum the t_2 duration is kept constant at its minimum value and receiver = $4(x)$, $8(-x)$, $4(x)$, with all rf pulse phases unchanged. Quadrature detection in the t_1 and t_2 dimensions is obtained by altering the phases ϕ_1 and ϕ_4, respectively, in the regular states-TPPI manner. RF power: ^1H, $\gamma_H B_1 = 27$ kHz (high-power pulses), 220 Hz (low-power pulses), 3.1 kHz (Waltz-16); ^{15}N, $\gamma_N B_2 = 5.3$ kHz, or 1.0 kHz (Waltz-16); $^{13}C'$, $\gamma_C B_2 = 4.5$ and 4.0 kHz at 151 and 126 MHz; $^{13}C^{\alpha/\beta}$, sine-bell-shaped 180° pulses of 180 μs (126 MHz) or 150 μs (151 MHz). Carrier position: ^1H, H_2O (4.79 ppm); $^{13}C'$, 177 ppm; ^{15}N, 116.5 ppm. Delay durations: $\tau = 2.25$ ms; $\Delta = 5.4$ ms; $T = 13.8$ ms; $T' = 12.5$ ms; $\delta = 56.1$ ms. Acquisition of the 3D reference spectrum utilizes the same phase cycle and timing parameters as listed above, except for a shorter duration of δ ($\delta' = 46.7$ ms), and a 4 times narrower spectral width in the t_2 dimension. Gradients (sine-bell-shaped; 25 G/cm at center): $G_{1,2,3,4,5,6} = 3.75$, 1.5, 0.5, 1.65, 1.35, and 0.5 ms. The inset shows a polypeptide backbone fragment in which dashed lines connect the pairs of nuclei for which J_{CC} couplings can be measured.

The total measuring time for the 2D reference spectrum was 27 min. For both data sets, acquired data were apodized with a 60°-shifted squared sine-bell in the H^N dimension, truncated at 10%, with a 55°-shifted sine-bell in the $^{13}C'$ dimension, truncated at 5%, and with an untruncated squared cosine-bell in the t_1 dimension after mirror-image linear prediction[17] (12 coefficients) was used to extend the data to 64* points. The first two data points in the $^{13}C'$ dimension are not acquired with the scheme of Figure 1 and were reconstructed using linear prediction, making the total length of the time domain 8.2 ms. Data were zero-filled to yield a digital resolution of 10.9 (F_1), 39.1 (F_2), and 4.4 Hz (F_3).

The 3D HN(CO)C spectrum for apoCaM was recorded at 500 MHz as a 35* × 67* × 512* data matrix with acquisition times of 30.2 (t_1, ^{15}N), 8.0 (t_2, ^{13}C), and 63.9 ms (t_3, $^1H^N$). The total measuring time was 62 h. A 3D reference spectrum was recorded as a 35* × 17* × 512* data matrix with acquisition times of 30.2 (t_1, ^{15}N), 8.2 (t_2, ^{13}C), and 63.9 ms (t_3, $^1H^N$) using the same pulse scheme, but tuning the dephasing delay δ to 46.7 instead of 56.07 ms, such as to obtain maximum intensity one-bond correlations to C^α and a spectrum with the same appearance as a regular HN(CO)CA spectrum.[18] The total measuring time for the 3D reference spectrum was 16 h. For both data sets, acquired data were apodized with a 60°-shifted squared sine-bell in the t_3 dimension, truncated at 10%, with a 55°-shifted sine-bell in the t_2 dimension, truncated at 5%, and with an untruncated squared cosine-bell in the t_1 dimension after mirror-image linear prediction (12 coefficients) was used to extend the data to 55* points. Data were zero-filled to yield a digital resolution of 9.0 (F_1), 32.5 (F_2), and 7.8 Hz (F_3). Data were processed using the package NMRPipe.[19] Peak

(13) Brünger, A. T. *X-PLOR Version 3.1: A System for X-ray Crystallography and NMR*; Yale University Press: New Haven, CT, 1992.
(14) Head-Gordon, T., Head-Gordon, M., Frisch, M. J., Brooks, C. L., III; Pople, J. A. *J. Am. Chem. Soc.* **1991**, *113*, 5989−5997.
(15) Edison, A. S., Weinhold, F., Westler, W .M., Markley, J. L. *J. Biomol. NMR* **1994**, *4*, 543−551.
(16) Sulzbach, H. M.; Schleyer, P. v. R.; Schaefer, H. F., III. *J. Am. Chem. Soc.* **1995**, *117*, 2632−2637.
(17) Zhu, G.; Bax, A. *J. Magn. Reson.* **1992**, *100*, 202−207.
(18) Bax, A.; Ikura, M. *J. Biomol. NMR* **1991**, *1*, 99−104.
(19) Delaglio, F.; Grzesiek, S.; Vuister, G. W.; Zhu, G.; Pfeifer, J.; Bax, A. *J. Biomol. NMR* **1995**, *6*, 277−293.

positions and intensities were determined interactively using polynomial interpolation with the program PIPP.[20]

Resonance assignments follow those reported previously for apo-CaM[11] and human ubiquitin.[21−23] Ubiquitin C^{γ} resonance assignments were obtained from the HN(CO)C experiment described in this work and agree with data recently reported by Wand et al.[24]

Results and Discussion

The peptide torsion angle ϕ is characterized by six three-bond J couplings: $^3J_{HNH^{\alpha}}$, $^3J_{HNC'}$, $^3J_{HNC^{\beta}}$, $^3J_{C'H^{\alpha}}$, $^3J_{C'C'}$, and $^3J_{C'C^{\beta}}$. Details regarding the methods for measuring the first five couplings, including their values in human ubiquitin, have been presented previously.[9,12] In the present study we describe an experiment for measuring $^3J_{C'C^{\beta}}$. In addition, this experiment yields quantitative $^3J_{C'C^{\gamma}}$ couplings, related to the χ_1 torsion angles, and two two-bond couplings, $^2J_{C'C^{\beta}}$ and $^2J_{C'C^{\alpha}}$.

Description of the Pulse Scheme. The pulse sequence for measuring $^3J_{C'C^{\beta}}$ and $^3J_{C'C^{\gamma}}$ couplings is shown in Figure 1. The pulse scheme is virtually identical to that of the regular HN-(CO)CA experiment, and the magnetization transfer in this class of experiments has been discussed in detail elsewhere.[18,25,26] Therefore, the discussion focuses primarily on aspects relevant for quantitative measurement of $J_{C'C}$ from such spectra.

Magnetization is first transferred from the amide proton (H^N) to the ^{15}N (at time point *a*) and on to its preceding $^{13}C'$ (at time point *b*). During the subsequent $2\delta + t_2$ interval, between time points *b* and *e*, $^1J_{NC'}$ may be ignored as the dephasing effect of this coupling is refocused by the $180^{\circ}_{\phi_5}$ $^{13}C'$ pulse. Homonuclear $^{13}C'-^{13}C'$ J dephasing occurs during the entire $2\delta + t_2$ interval, however, and modulates the C'_yN_z magnetization at time point *e* by $\Pi_k\cos[\pi J_{C'C^k}(2\delta + t_2)]$, where the product extends over all carbonyl/carboxyl carbons, *k*, coupled to the $^{13}C'$ of interest. With the exception of Asp and Asn residues (*vide infra*), where the intraresidue coupling to the carboxyl/carbonyl $^{13}C^{\gamma}$ can be large (~5 Hz for $\chi_1 \approx -60°$), this product does not deviate much from unity and merely causes a small attenuation of resonance intensity observed in the 3D spectrum (and a similar attenuation of the 2D reference spectrum, *vide infra*).

During the delay δ, immediately following time point *b*, C'_yN_z magnetization dephases with respect to its aliphatic ^{13}C coupling partners, *p* and *q*:

$$C'_yN_z \rightarrow C'_yN_z\Pi_p\cos(\pi J_{C'C^p}\delta) - \Sigma_q 2C'_xC^q_zN_z\sin(\pi J_{C'C^q}\delta)\Pi_{p\neq q}\cos(\pi J_{C'C^p}\delta) + \ldots \quad (1)$$

where ... refers to terms where C' is antiphase with respect to two or more aliphatic carbons, and chemical shift evolution has been omitted to simplify the expression. The duration of δ is carefully chosen to correspond to an integral multiple of $(^1J_{C'C^{\alpha}})^{-1}$, such that C' is in-phase with respect to C^{α} at time point *c*. Note that in proteins $^1J_{C'C^{\alpha}}$ has a very uniform value of 54 ± 1 Hz. The terms in eq 1 where C' is antiphase with respect to two aliphatic carbons are eliminated by the phase cycle of the $90^{\circ}_{\phi_4}$ pulse, and to first order, they do not affect the measurement of $J_{C'C^q}$. Higher order terms, where C' becomes antiphase with respect to more than two aliphatic carbons, in practice are vanishingly small and may safely be ignored. The term containing the operator product $C'_xC^q_zN_z$ is converted into $C'-C^q$ multiple quantum coherence by the $90^{\circ}_{\phi_4}$ pulse (time point *c*) and gives rise to a C^q cross-peak in the F_2 dimension of the 3D spectrum. After the t_2 evolution period, this term is converted back into $C'_xC^q_z\,N_z$ magnetization (time point *d*) and subsequently rephases during the second δ delay:

$$2C'_xC^q_zN_z\sin(\pi J_{C'C^q}\delta)\Pi_{p\neq q}\cos(\pi J_{C'C^p}\delta) \rightarrow C'_yN_z\sin^2(\pi J_{C'C^q}\delta)\Pi_{p\neq q}\cos^2(\pi J_{C'C^p}\delta) \quad (2)$$

Thus, the net observed H^N magnetization in the 3D experiment, t_2-modulated by ω_{C^q}, is proportional to $\sin^2(\pi J_{C'C^q}\delta)\Pi_{p\neq q}\cos^2(\pi J_{C'C^p}\delta)$. In order to derive $J_{C'C^q}$ from this intensity, a second, so-called reference spectrum is recorded. In its simplest form, this simply involves alteration of the phase cycle of the pulse scheme in Figure 1, such that only the magnetization component which is not subject to J dephasing during each of the δ delays is selected, yielding

$$C'_yN_z \rightarrow C'_yN_z\Pi_p\cos^2(\pi J_{C'C^p}\delta) \quad (3)$$

This component is not modulated as a function of t_2 and is therefore most easily measured in a 2D version of the experiment, in which only t_1 (and not t_2) is incremented. The relative intensity of the cross-peak with C^q, I_C, and the corresponding peak in the 2D reference spectrum, I_{ref}, then equals

$$I_C/I_{ref} = \tan^2(\pi J_{C'C^q}\delta)F_{\omega_2}N_2 \quad (4)$$

where F_{ω_2} accounts for the difference between recording 2D and 3D spectra, and N_2 is the number of complex increments in the t_2 dimension.[27] In case there is only a single modulation frequency in the t_2 dimension, $F_{\omega_2}N_2$ equals the ratio of the C^q cross-peak intensity over the intensity of the first time domain point in the t_2 dimension of the 3D experiment. The value of F_{ω_2} depends on the digital filtering function used, the T_2 of the $^{13}C^q$ resonance, and the number of ^{13}C nuclei attached to it. Provided the acquisition time in the t_2 dimension is shorter than $(2^1J_{CC})^{-1} \approx 15$ ms, one-bond $^{13}C-^{13}C$ splittings will not be resolved and F_{ω_2} is relatively insensitive to the number of ^{13}C nuclei attached to it, and to its T_2 value. The applicable F_{ω_2} value is obtained most easily by computer simulation and F_{ω_2} values applicable for an acquisition time of 8.2 ms and a range of T_2 values and different numbers of attached ^{13}C nuclei are given in Table 1. As can be seen from this table, the effects of differences in ^{13}C relaxation rates are relatively small (owing to the short acquisition time in the t_2 dimension), and a rough estimate of T_2 generally will not introduce errors larger than ~5% in F_{ω_2}, resulting in an error contribution in the final $J_{C'C^q}$ value of less than ~2.5%.

The equations presented above assume that the spin state of the aliphatic carbons remains unchanged between time points *b* and *e* in Figure 1. However, for the relatively rapidly tumbling ubiquitin protein, ^{13}C T_1 values at 151 MHz are expected to fall in the 0.25−1 s range. Correcting for this finite ^{13}C T_1 is straightforward[28] and increases $J_{C'C^q}$ by ~10% for $T_1 = 0.25$ s and ~2% for $T_1 = 1$ s. As the ^{13}C T_1 values for the backbone

(20) Garrett, D. S.; Powers, R.; Gronenborn, A. M.; Clore, G. M. *J. Magn. Reson.* **1991**, *95*, 214−220.
(21) Di Stefano, D. L; Wand, A. J. *Biochemistry* **1987**, *26*, 7272−7281.
(22) Weber, P. L.; Brown, S. C.; Mueller, L. *Biochemistry* **1987**, *26*, 7282−7290.
(23) Wang, A. C.; Grzesiek, S.; Tschudin, R.; Lodi, P. J.; Bax, A. *J. Biomol. NMR* **1995**, *5*, 376−382.
(24) Wand, A. J.; Urbauer, J. L.; McEvoy, R. P.; Bieber, R. J. *Biochemistry* **1996**, *35*, 6116−6125.
(25) Grzesiek, S.; Bax, A. *J. Magn. Reson.* **1992**, *96*, 432−440.
(26) Cavanagh, J.; Fairbrother, W.; Palmer, A. G., III; Skelton, N. J. *Protein NMR Spectroscopy*; Academic Press: San Diego, CA, 1996; pp 491−494.
(27) Vuister, G. W.; Yamazaki, T.; Torchia, D. A.; Bax, A. *J. Biomol. NMR* **1993**, *3*, 297−306.
(28) Vuister, G. W., Bax, A. *J. Am. Chem. Soc.* **1993**, *115*, 7772−7777. Kuboniwa, H., Grzesiek, S., Delaglio, F., Bax, A. *J. Biomol. NMR* **1994**, *4*, 871−878.
(29) Dayie, K. T.; Wagner, G. *J. Magn. Reson.* **1995**, *109*, 105−108.

Table 1. Scaling Factors for Correlating Intensity in a 3D HN(CO)C Spectrum to That in a 2D Spectrum

T_2^a (ms)	m^b	$F_{\omega_2}{}^c$	T_2^a (ms)	m^b	$F_{\omega_2}{}^c$
40.0	0	0.683	25.0	0	0.651
40.0	1	0.630	25.0	1	0.603
40.0	2	0.586	25.0	2	0.563
40.0	3	0.550	25.0	3	0.528

[a] Transverse relaxation time of side chain ^{13}C. [b] Number of ^{13}C nuclei attached to the carbon of interest. [c] $F_{\omega_2} = (1/N_2)\Sigma_{n=1,\ldots,N_2} \exp(-n\Delta t_2/T_2) \cos^m(\pi J_{CC} n\Delta t_2)\, G(n\Delta t_2)$, where N_2 represents the number of complex data points sampled in the t_2 dimension, Δt_2 is the t_2 increment, and $G(n\Delta t_2)$ is the applied digital filtering function. F_{ω_2} values have been calculated for a time domain length, AT, of 8 ms, $J_{CC} = 35$ Hz, and $G(n\Delta t_2) = \sin[0.45\pi + 0.5\pi n\Delta t_2/\mathrm{AT}]$. Thus, the scale factor $N_2F_{\omega_2}$ needs to be used when intensities are compared in the 2D reference spectrum and the 3D spectrum. Note that for most Fourier transform algorithms the scale factor is independent of zero filling, except for a possible small increase in peak height resulting from better digitization of the spectrum.

^{13}C$^\alpha$ atoms in ubiquitin exhibit extensive variations,[24] and no T_1 values for non-methyl side chain carbons in ubiquitin have been reported, no correction is made. Values reported in this study therefore underestimate the true $J_{C'C}$ long-range couplings by up to 10%.

In deriving eqs 1−4, the effect of $^3J_{C'C'}$ couplings has been ignored. These couplings will attenuate both the 3D and the 2D reference spectra by the same factor, Q, given by

$$Q = \Pi_m \cos(2\pi^3 J_{C'C^{m'}}\delta) \qquad (5)$$

where the product extends over all carbonyl and carboxyl carbons coupled to C′. $^3J_{C'C'}$ couplings among backbone carbons are invariably small,[9] and the term Q for typical values of δ is close to 1. However, for Asp and Asn residues with $\chi_1 = -60°$, corresponding to a C′−C$^\gamma$ J coupling of ∼5 Hz, this term can result in disappearance of the resonance from both the reference spectrum and the 3D HN(CO)C spectrum.

For quantitative measurement in proteins where the 2D ^{1}H−^{15}N reference spectrum, obtained with the pulse scheme of Figure 1, is insufficiently resolved, a 3D reference spectrum may be recorded in the following manner. By shortening the value of δ used in the HN(CO)C experiment by $(2\ ^1J_{C'C^\alpha})^{-1} \approx$ 9.26 ms, one obtains a 3D HN(CO)CA reference spectrum. The intensity ratio of a long-range correlation to C^q and the C$^\alpha$ cross-peak in the 3D reference spectrum is given by

$$I_C/I_{\mathrm{ref}} = [\sin^2(\pi J_{C'C^q}\delta)\Pi_{p\neq q}\cos^2(\pi J_{C'C^p}\delta) N_2 F^q{}_{\omega_2} \times \exp[-2(\delta - \delta')/T_{2C'}]/[\, F^\alpha{}_{\omega_2}\Pi_p \cos^2(\pi J_{C'C^p}\delta') N_2'] \quad (6)$$

where $\delta' = \delta - (2\ ^1J_{C'C^\alpha})^{-1}$, $T_{2C'}$ is the C′ T_2 value, and $F^q{}_{\omega_2}$ and $F^\alpha{}_{\omega_2}$ are the functions accounting for the shape of the time domain data in the t_2 dimension (Table 1). The product in the denominator extends over all aliphatic carbons except the intraresidue C$^\alpha$, and eq 6 assumes that $\sin(\pi J_{C'C^\alpha}\delta') = 1$. In the reference 3D spectrum, only correlations to C$^\alpha$ have nonvanishing intensities, and the spectral window in the t_2 dimension may be reduced accordingly while the acquisition time is kept the same, resulting in a lower number of data points, N_2', and a shorter total measuring time for the reference spectrum. The term $\exp[-2(\delta - \delta')/T_{2C'}]$ in eq 6 is unknown, but a reasonable estimate can be made on the basis of the protein's rotational correlation time.[30] Considering the small value of $\delta - \delta'$, a rough estimate for $T_{2C'}$ suffices, and small errors in $T_{2C'}$ do not significantly affect quantitative measurement of $J_{C'C^q}$. Excluding flexible backbone regions and ^{13}C′ resonances subject to slow or intermediate time scale conformational exchange, the $T_{2C'}$ value may be approximated by $1/T_{2C'} \approx \tau_c(3/4 + B^2/150)\ \mathrm{s}^{-1}$, where τ_c is the rotational correlation time in nanoseconds, and B the magnetic field strength in tesla.

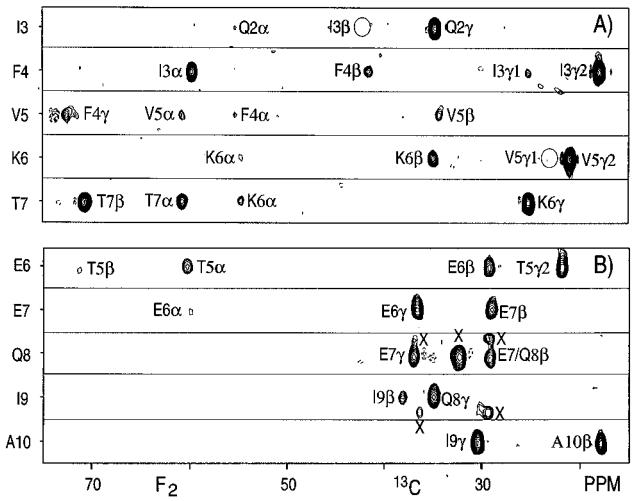

Figure 2. (F_2, F_3) strips from the 3D HN(CO)C spectrum of (A) 1.8 mM ^{13}C/^{15}N-enriched ubiquitin (pH 4.7; 30 °C; 600 MHz), taken at the ^{1}H^N (F_3) and ^{15}N (F_1) frequencies of Ile^3−Thr^7, and (B) 1.3 mM apoCaM (pH 6.3; 23 °C; 500 MHz), taken at the ^{1}H^N/^{15}N frequencies of Glu^6−Ala^{10}. Open circles mark the locations of cross-peaks which as a result of small $^3J_{C'C^\beta}$ and $^3J_{C'C^\gamma}$ values fall below the noise threshold. Correlations from residues with ^{1}H^N/^{15}N frequencies in the vicinity of the selected strips are marked "X". The ubiquitin Phe^4-C$^\gamma$ resonance is aliased and dispersive.

Measurement of $^3J_{C'C^\beta}$ and $^3J_{C'C^\gamma}$. For each amide, i, up to five cross-peaks can be observed in the 3D HN(CO)C experiment. They correspond to a usually vanishingly weak cross-peak to C$^\alpha$ of residue $i - 1$ (resulting from small deviations from the condition $\delta = N/^1J_{C'C^\alpha}$), $C^\alpha{}_i$ and $C^\beta{}_{i-1}$, resulting from the two-bond couplings $^2J_{C'C^\alpha}$ and $^2J_{C'C^\beta}$, and $C^\gamma{}_{i-1}$ and $C^\beta{}_i$, which result from the $^3J_{C'C^\gamma}$ and $^3J_{C'C^\beta}$ couplings of interest.

Figure 2A shows an example of the cross-peaks observed for the amides of residues Ile^3−Thr^7 in ubiquitin. As a result of ubiquitin's short rotational correlation time (4.1 ns),[30] its ^{1}H, ^{15}N, and ^{13}C transverse relaxation times are relatively long, and the experiment yields a spectrum with a high signal-to-noise ratio. Quantitative values for the $J_{C'C^q}$ couplings have been derived from the cross-peak intensities, using eq 4 and a 2D reference spectrum, recorded in the manner described above. The J values are presented in Table 1 of the Supporting Information.

Since the experiment has been optimized to observe correlations from ^{13}C′ to aliphatic carbons by positioning the aliphatic carbon excitation frequency at about 45 ppm, correlations to ^{13}C$^\gamma$ of Asp and Asn are not observed. However, if the χ_1 angle of these residues is −60°, corresponding to a *trans* $^3J_{C'C^\gamma}$ coupling of *ca.* 5 Hz, the $\cos(2\pi^3 J_{C'C^{m'}}\delta)$ factor in eq 5 can become very small or even negative. As a result, the intensity of the amide following this Asp or Asn residue in the reference spectrum will also become very weak or negative. For example, the amides of the residues following Asp^{21} and Asp^{58} in ubiquitin are weak and of opposite sign in the reference spectrum (data not shown), indicating that $^3J_{C'C^\gamma} > 1/(4\delta) = 4.5$ Hz, or $\chi_1 \approx -60°$ for these residues.

^{13}C$^\gamma$ resonances of aromatic residues also fall well outside the optimal excitation region for the rectangular aliphatic ^{13}C pulses, which are adjusted to have a null in their excitation

(30) Schneider, D. M., Dellwo, M. J. and Wand, A. J. *Biochemistry* **1992**, *31*, 3645−3652. Tjandra, N.; Feller, S. E.; Pastor, R. W.; Bax, A. *J. Am. Chem. Soc.* **1995**, *117*, 12562−12566.

profile at the $^{13}C'$ frequency. Nevertheless, correlations to aromatic resonances can be observed, albeit attenuated as a result of nonoptimal excitation, and they appear as aliased, out-of-phase resonances in the 3D HN(CO)C spectrum. For example, the amide of Val[5] in Figure 2A shows a correlation to the aliased $^{13}C^{\gamma}$ of Phe[4]. Quantitative values for $^3J_{C'C^{\gamma}}$ (and $^3J_{NC^{\gamma}}$) of aromatic residues are obtained most easily using a recently described two-dimensional spin-echo difference experiment.[31]

Figure 2B shows five strips for the amides of Glu[6]−Ala[10] in apoCaM. Due to the longer rotational correlation time (*ca*. 8 ns),[11] transverse relaxation times are considerably shorter than in ubiquitin, and the sensitivity of the experiment is correspondingly lower. On average, only $J_{C'C^{q}}$ couplings larger than *ca*. 1 Hz give rise to an observable cross-peak. For each of the five amides shown, the intraresidue $^{13}C^{\beta}$ and the $^{13}C^{\gamma}$ of the preceding residue are observed, indicating relatively large values for the corresponding $^3J_{C'C^{\beta}}$ and $^3J_{C'C^{\gamma}}$ couplings. As will be discussed below, large values for $^3J_{C'C^{\beta}}$ correspond to $\phi \approx -60°$, and large values for $^3J_{C'C^{\gamma}}$ indicate $\chi_1 \approx -60°$, in agreement with the previously determined side chain angles and α-helical backbone geometry for these residues.[32] Quantitative $^3J_{C'C^{\gamma}}$ and $^3J_{C'C^{\beta}}$ values for apo-CaM have been obtained by using a 3D HN(CO)CA spectrum as a reference (*cf.* eq 6), and results are summarized in Table 2 of the Supporting Information.

Parametrization of $^3J_{C'C^{\beta}}$ Karplus Equation. Previously, Kao and Barfield[33] reported $^3J_{C'C}$ values in C′−N−C−C *cis*-form model compounds, and a Karplus curve appropriate for peptides relating $^3J_{C'C^{\beta}}$ couplings to backbone ϕ angles has been proposed on the basis of FPT-INDO calculations.[2] Here, we present the first empirical Karplus relation for this coupling, based on $^3J_{C'C^{\beta}}$ couplings measured for ubiquitin and ϕ angles from its X-ray structure.[10]

$^3J_{C'C^{\beta}}$ couplings measured in ubiquitin fall in the 0.54−2.78 Hz range. Figure 3 shows the relation between these couplings and the corresponding crystal structure ϕ angles. A best fit of the measured values to a Karplus equation,[1,2] $J = A\cos^2\theta + B\cos\theta + C$, is calculated using singular value decomposition (SVD), yielding

$$^3J_{C'C^{\beta}} = 1.61\cos^2(\phi - 120°) - 0.66\cos(\phi - 120°) + 0.26\ \text{Hz} \quad (7)$$

Except for a small offset, the present parametrization (thick solid line in Figure 3) is remarkably similar to the curve obtained from FPT-INDO calculations[2] (thin solid line).

Three-bond *J* couplings are dominated by the Fermi contact contribution, and usually only the valence s orbital contributions, which have the highest electron densities at the nuclei, have been considered. However, for *J* couplings across peptide bonds, π-orbitals in principle also could be significant.[34,35] Orbital hybridization potentially could also introduce a very small contribution from 2p orbitals of sp^3-hybridized carbons to the *J* coupling, and in addition, mechanisms other than the Fermi contact contribution may not be entirely negligible.[35,36] In order to rule out the possibility that these mechanisms introduce a phase shift in the $^3J_{C'C^{\beta}}$ parametrization of eq 7, we have also fit the data as a function of such a phase shift. As shown in the Supporting Information, both for $^3J_{C'C'}$ and $^3J_{C'C^{\beta}}$, the best fit to the crystal structure is obtained when this phase shift is extremely small (−0.5° for $^3J_{C'C^{\beta}}$) or zero (for $^3J_{C'C'}$). This indicates that no systematic errors in the torsion angles will be introduced when these *J* couplings are used for structure calculation.

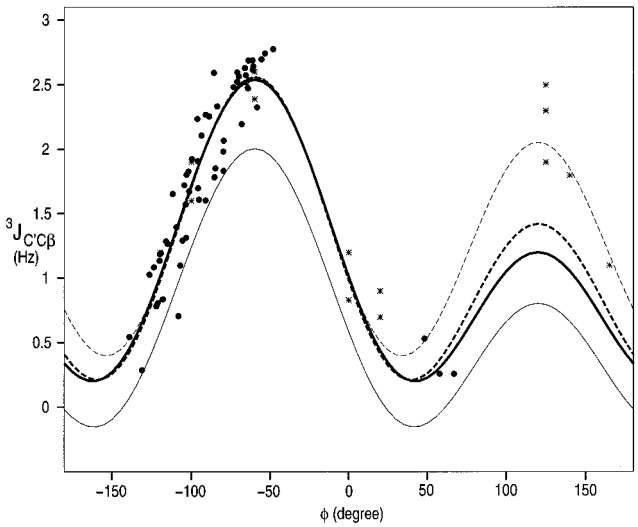

Figure 3. Relation between $^3J_{C'C^{\beta}}$ and the protein backbone angle ϕ. Solid circles represent measured $^3J_{C'C^{\beta}}$ values as a function of the crystallographically determined ϕ angle; asterisks correspond to previously reported $^3J_{CC}$ values in conformationally constrained model compounds containing the analog of a *cis* peptide bond.[33] Lines correspond to Karplus equations of the type $J = A\cos^2(\phi - 120°) + B\cos(\phi - 120°) + C$ Hz. The thick solid line represents the best fit between $^3J_{C'C^{\beta}}$ and the crystallographically determined ϕ angles ($A = 1.61 \pm 0.10$; $B = -0.66 \pm 0.05$; $C = 0.26 \pm 0.02$). The thick dashed line is the best fit using ϕ angles derived from $^3J_{HNH^{\alpha}}$, $^3J_{HNC^{\beta}}$, $^3J_{HNC'}$, $^3J_{C'H^{\alpha}}$, and $^3J_{C'C'}$ ($A = 1.74 \pm 0.06$; $B = -0.57 \pm 0.03$; $C = 0.25 \pm 0.02$). The thin dashed line includes the data points measured by Kao and Barfield[33] in the fit, and using crystal structure ϕ angles for the ubiquitin residues ($A = 1.9$; $B = -0.25$; $C = 0.4$). The thin solid line represents the curve obtained from FPT-INDO calculations ($A = 1.5$; $B = -0.6$; $C = -0.1$).[2]

All peptide bonds in ubiquitin are *trans*. However, except for the region where $\phi \approx +120°$, the values previously measured for C′−N−C−C *cis*-form model compounds[33] (asterisks in Figure 3) fall close to the curve of eq 7. This indicates that, at least for negative ϕ angles, $^3J_{C'C^{\beta}}$ is not sensitive to the *cis* or *trans* state of the peptide bond. Because ϕ angles near +120°, corresponding to *cis* C′−C^{β} couplings, do not occur in proteins for steric reasons, the value of the Karplus equation in this region is ill-determined by eq 7. The *cis* values reported by Kao and Barfield also have relatively large uncertainties as these values include subtraction of an estimated two- or three-bond *J* coupling contribution.[33] A parametrization which includes the J_{CC} values of Kao and Barfield yields the following Karplus coefficients: $A = 1.90$; $B = -0.25$; $C = 0.40$ (thin dashes in Figure 3).

The rmsd between measured $^3J_{C'C^{\beta}}$ values and those predicted by eq 7 is 0.24 Hz when using ϕ angles from the crystal structure. The rmsd drops to 0.17 when ϕ angles derived from $^3J_{HNH^{\alpha}}$, $^3J_{HNC^{\beta}}$, $^3J_{HNC'}$, $^3J_{H^{\alpha}C'}$, and $^3J_{C'C'}$ are used instead, resulting in a noticeable change in Karplus parameters, with $A = 1.74$, $B = -0.57$, and $C = 0.25$. However, as can be seen from Figure 4, this latter Karplus curve (thick dashed line) is nearly indistinguishable from eq 7 in the populated region of the curve ($\phi < -50°$).

(31) Hu, J.-S.; Grzesiek, S.; Bax, A. *J. Am. Chem. Soc.*, **1997**, *119*, 1803−1804.
(32) Zhang, M., Tanaka, T., Ikura, M. *Nat. Struct. Biol.* **1995**, *2*, 758−767; Kuboniwa, H.; Tjandra, N.; Grzesiek, S.; Ren, H.; Klee, C. B.; Bax, A. *Nat. Struct. Biol.* **1995**, *2*, 768−776.
(33) Kao, L.-F.; Barfield, M. *J. Am. Chem. Soc.* **1985**, *107*, 2323−2330.
(34) Wasylishen, R. E.; Schaefer, T. *Can. J. Chem.* **1973**, *51*, 1906−1909.
(35) Fukui, H. *Nucl. Magn. Reson. Spec. Periodic Rep.* **1994**, *24*, 133−161; Parella, T.; Sanchez-Ferrando, F.; Virgili, A. *Magn. Reson. Chem.* **1997**, *35*, 30−34.
(36) Edison, A. S.; Markley, J. L.; Weinhold, F. *J. Phys. Chem.* **1993**, *97*, 11657−11665.

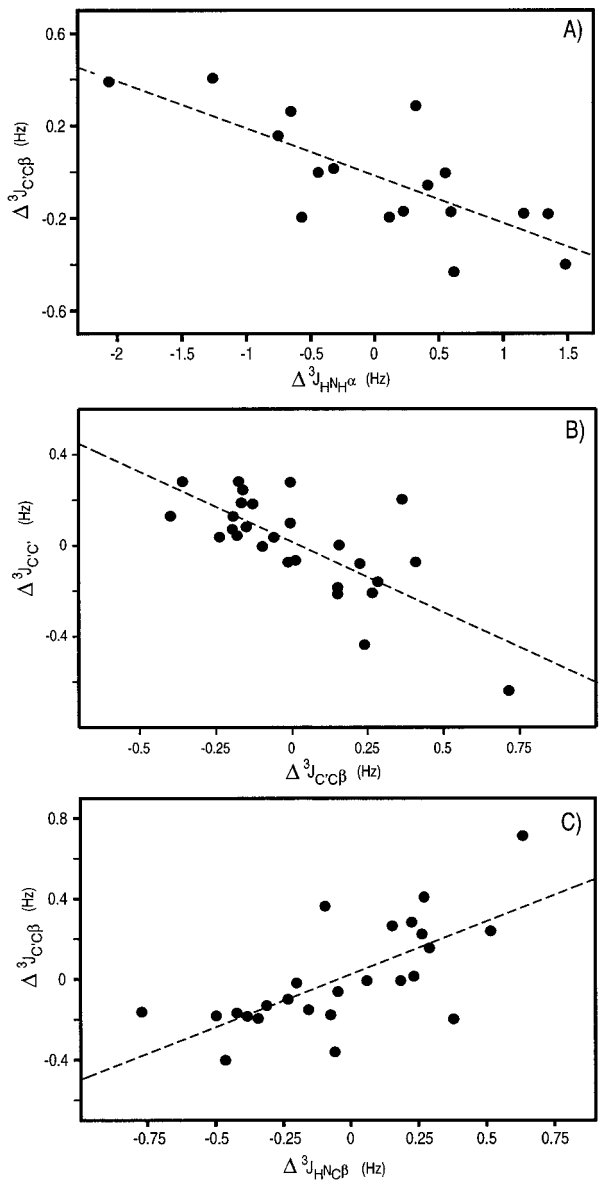

Figure 4. Correlation plot of the difference between measured *J* values and values predicted by the Karplus equation on the basis of the ubiquitin crystal structure ϕ angles, $\Delta J = J_{meas} - J_{pred}$, for (A) $^3J_{H^NH^\alpha}$ and $^3J_{C'C^\beta}$ in the range $-105° \le \phi \le -85°$, (B) $^3J_{C'C^\beta}$ and $^3J_{C'C'}$ in the range $-130° \le \phi \le -90°$, and (C) $^3J_{C'C^\beta}$ and $^3J_{H^NC^\beta}$ in the range $-120° \le \phi \le -90°$. For residues in the selected ranges, both *J* couplings have a strong, nearly-linear dependence on ϕ. The statistical significance of these correlations[42] is described by the correlation coefficients, *r*, defined by $r = \sum_i[(x_i - x_{av})(y_i - y_{av})]/[\sum(x_i - x_{av})^2\sum(y_i - y_{av})^2]^{1/2}$. These *r* values are (A) 0.76, (B) 0.73, and (C) 0.70, and the conditional probabilities, *P*, that these correlations result from random uncertainties are 4×10^{-4}, 1.5×10^{-5}, and 1×10^{-4}, respectively.

If the difference between measured *J* values and those predicted by eq 7, $\Delta J(\phi) = J_{meas}(\phi) - J_{pred}(\phi)$, is dominated by the uncertainty in the ϕ angle, $\Delta J(\phi)$ values for the different types of ϕ-dependent *J* values are expected to be strongly correlated with one another. Such strong correlations are indeed observed: For example, Figure 4A compares the deviations between measured $^3J_{HNH^\alpha}$ and $^3J_{C'C^\beta}$ values and the values predicted by their respective Karplus curves (using crystal structure ϕ angles) for residues with $-105° < \phi < -85°$, i.e., for a set of residues where both Karplus curves have a strong ϕ dependence. Similarly strong correlations are observed when the deviations between measured and predicted values for $^3J_{C'C^\beta}$ are compared with those for $^3J_{C'C'}$ (Figure 4B) or with the ones for $^3J_{HNC^\beta}$ (Figure 4C). Note that, for planar peptide bonds, the $H^N-N-C^\alpha-C^\beta$ and the $C'-N-C^\alpha-C^\beta$ dihedral angles differ by 180°, and the strongest ϕ dependence of the two Karplus curves therefore is observed for the same range of ϕ angles ($-130° < \phi < -90°$). These data therefore indicate that the rms random error in the measured $^3J_{C'C^\beta}$ values is considerably smaller than 0.24 Hz and confirms our previous finding[12] that small differences between the crystal structure ϕ angles and those present in the solution state are a major cause for the difference between measured and predicted *J* values.

Previously, the ϕ values in ubiquitin were recalculated on the basis of the values of $^3J_{HNH^\alpha}$, $^3J_{HNC^\beta}$, $^3J_{HNC'}$, and $^3J_{H^\alpha C'}$, resulting in a rmsd of 7.0° relative to the angles in the crystal structure.[12] Following the same procedure, but also adding the $^3J_{C'C'}$ and $^3J_{C'C^\beta}$ couplings, yields a new set of ϕ angles (Supporting Information) which are very close to the previous NMR derived angles and differs by a similar amount (rmsd = 6.6°) from the crystal structure.

A second indicator for the high degree of consistency among the complementary *J* couplings can be obtained by using all but one of the observed *J* couplings to derive the ϕ angle, and then to use the Karplus equation for the remaining *J* coupling to predict its value. For 57 residues at least five ϕ angle related *J* couplings were measured. For each of these 57 residues, a ϕ angle is calculated which minimizes $\Sigma[J_{meas} - J_{pred}(\phi)]^2/E_{J_{meas}}{}^2$, where the summation extends over $^3J_{HNH^\alpha}$, $^3J_{HNC^\beta}$, $^3J_{HNC'}$, $^3J_{C'C'}$, and $^3J_{H^\alpha C'}$. $E_{J_{meas}}$ is the standard deviation between the measured *J* values and the Karplus curve (0.70, 0.30, 0.45, 0.17, and 0.29 Hz, respectively), and planar peptide bond geometry is assumed. This new set of ϕ values is then used to predict $^3J_{C'C^\beta}$. The rmsd between the thus predicted and measured $^3J_{C'C^\beta}$ values is only 0.16 Hz, considerably smaller than the 0.24 Hz rmsd between the measured $^3J_{C'C^\beta}$ and the value predicted by the crystallographic ϕ angles. Similarly, if $^3J_{HNC^\beta}$, $^3J_{HNC'}$, $^3J_{C'C'}$, $^3J_{C'H^\alpha}$, and $^3J_{C'C^\beta}$ are used to derive ϕ angles for predicting $^3J_{HNH^\alpha}$, this yields a rmsd of 0.39 Hz between measured and calculated values, *versus* 0.70 Hz between the measured $^3J_{HNH^\alpha}$ values and the ones predicted on the basis of the crystallographic ϕ angles. Karplus parameters for all six ϕ-related ^3J couplings, obtained in this manner using these solution ϕ angles for the 57 residues for which at least five ϕ-related *J* couplings were measured, are summarized in Table 2.

Planarity of the Peptide Bond. *Ab initio* calculations for dipeptide analogs in vacuum suggest large deviations from planarity for the peptide bond, depending on the values of the backbone angles ϕ and ψ.[14,15] Similarly, calculations of $^{13}C'$ chemical shifts only agree with the experimentally observed values if significant pyramidalization at the peptide N is introduced, in particular for α-helical residues.[16] If the peptide bond is nonplanar, and the $H^N_i-N_i-C^\alpha_i$ plane makes an angle θ with the $C'_{i-1}-N_i-C^\alpha_i$ plane, the dihedral angles between H^N_i and C^β_i, C'_i, and H^α_i differ by $180° + \theta$ from the corresponding dihedral angles between C'_{i-1} and C^β_i, C'_i, and H^α_i. As *J* values for all six couplings are available for 45 ubiquitin residues, we can verify experimentally whether θ differs by a statistically significant amount from zero. Thus, for each residue the ϕ angle is derived from the three *J* couplings involving C'_{i-1}, resulting in a set of angles $\phi(C'_{i-1})$, and from the three *J* couplings involving H^N_i, yielding $\phi(H^N)$. The ϕ angle for a given residue is obtained by searching for the ϕ value which minimizes the difference between the measured *J* values and those predicted by the corresponding Karplus equations, normalized for the measurement error in each of these *J* values.[12]

Table 2. Coefficients of Karplus Equations, $J = A\cos^2(\phi + \theta) + B\cos(\phi + \theta) + C$[a]

	θ (deg)	A	B	C	ϕ	rmsd[d]
$^3J_{H^NH^\alpha}$	−60	+6.47	−1.43	+2.03	X-ray[b]	0.70
	−60	+7.09	−1.42	+1.55	solution[c]	0.39
$^3J_{H^\alpha C'}$	120	+3.63	−2.10	+1.29	X-ray	0.29
	120	+3.72	−2.18	+1.28	solution	0.24
$^3J_{H^NC^\beta}$	60	+2.71	−0.35	+0.05	X-ray	0.30
	60	+3.06	−0.74	+0.13	solution	0.21
$^3J_{H^NC'}$	180	+4.10	−1.08	+0.07	X-ray	0.45
	180	+4.29	−1.01	0.00	solution	0.32
$^3J_{C'C'}$	0	+1.35	−0.91	+0.61	X-ray	0.17
	0	+1.36	−0.93	+0.60	solution	0.13
$^3J_{C'C^\beta}$[e]	−120	+1.61	−0.66	+0.26	X-ray	0.24
	−120	+1.74	−0.57	+0.25	solution	0.16

[a] Karplus coefficients determined from singular value decomposition analysis. [b] Karplus coefficients derived using the ϕ(X-ray) angles.[10] [c] Karplus coefficients derived using the ϕ(solution) angles that yield best agreement between the ^3J values measured for a given residue and those predicted by the Karplus equations (derived using ϕ(XRAY)). For deriving a $^3J_{XY}$ Karplus relation from ϕ(solution) angles, $^3J_{XY}$ values were not used for deriving ϕ(solution). For 45 residues five ^3J couplings were used to determine ϕ(solution); for an additional 12 residues only four ^3J couplings were used. [d] Root-mean-square difference between measured J values and those predicted by the Karplus equation derived using either ϕ(XRAY) or ϕ(solution). [e] $^3J_{C'C^\beta}$ values have not been corrected for the finite $^{13}C^\beta$ T_1. True $^3J_{C'C^\beta}$ values and Karplus parameters are therefore ∼5% larger, assuming the average $^{13}C^\beta$ T_1 value is 400 ms (see the text).

The two sets of ϕ angles obtained in this manner are available as Supporting Information, together with the crystallographically determined ones, ϕ(XRAY). The pairwise rmsd between $\phi(C'_{i-1})$ and $\phi(H^N)$ equals 7.7°; the pairwise rmsd between $\phi(C'_{i-1})$ and ϕ(XRAY) is 7.9°, and the pairwise rmsd between $\phi(H^N)$ and ϕ(XRAY) is also 7.9°. The pairwise rmsd between $\phi(C'_{i-1})$ and $\phi(H^N)$ includes both the effect of $\theta \neq 0$ and the random errors in $\phi(C'_{i-1})$ and $\phi(H^N)$, resulting from factors other than ϕ influencing ^3J and from random errors in the J measurements. These latter uncertainties in the measured J values alone already result in errors of *ca.* 3° for $\phi(H^N)$ and *ca.* 5° for $\phi(C'_{i-1})$. Therefore, the lower limit ($\theta = 0$) expected for the rms difference between $\phi(C'_{i-1})$ and $\phi(H^N)$ equals $(5^2 + 3^2)^{1/2} \approx 5.8°$. The observed rmsd of 7.7° between $\phi(C'_{i-1})$ and $\phi(H^N)$ then indicates that the rms value of θ must be smaller than ∼5°.

The rms θ value predicted by the *ab initio* $\theta(\phi, \psi)$ surface[14] for the 45 ubiquitin residues equals 15°, which is clearly incompatible with our experimental results. The apparent discrepancy between the theoretical calculations and our experimental results may be attributed to the fact that the *ab initio* results were derived in vacuum, *i.e.*, in the absence of any hydrogen bonding. Hydrogen bonding is predicted to increase the double bond character of the C′−N bond, and thereby increase its planarity.[37,38] In this respect it is interesting to note that, on average, $^1H-^{15}N$ dipolar couplings in magnetically aligned ubiquitin yield improved agreement with dipolar couplings predicted on the basis of the X-ray structure, when H^N is moved out of the $C'_{i-1}-N_i-C^\alpha$ plane by an amount *ca.* 5 times smaller than predicted by the vacuum calculations.[39]

Search of databases containing crystal structure coordinates of small peptides and proteins, solved at high resolution, indicates that deviations from peptide bond planarity are noticeable and show a weak correlation between the $C^\alpha_{i-1}-C'_{i-1}-N_i-C^\alpha_i$ torsion angle, ω, and the handedness of the chain chirality.[38,40] Residues with $180° > \phi + \psi > 0°$ or $\phi+\psi < -180°$ are called left-handed and show an average ω angle of 178.1°. Residues outside this region of the Ramachandran map are right-handed and have an average ω angle of 180.1°.[38] Examining the small-peptide crystal structure library, and restricting the survey to *trans* peptide bonds between natural amino acids in linear peptides and cyclic peptides of six or more residues, MacArthur and Thornton[38] reported a rms deviation of 5.9° from $\omega = 180°$. They show that the angle, θ, between the $C'_{i-1}-N_i-C^\alpha_i$ and $C'_{i-1}-N_i-H^N_i$ planes correlates in a slightly nonlinear manner with the deviation from peptide bond planarity, $\omega - 180°$, and its magnitude, on average, is smaller. Our result, rms $\theta < \sim 5°$, therefore does not disagree with their finding that rms$(\omega - 180°) = 5.9°$.

Relation between $^3J_{C'C^\gamma}$ and χ_1. Values for nearly all $^3J_{C'C^\gamma}$ couplings in ubiquitin have been measured from the 3D HN(CO)C spectrum, and these values are reported in the Supporting Information. $^3J_{C'C^\gamma}$ couplings between carbonyl and methyl carbons are in excellent agreement (pairwise rmsd = 0.16 Hz) with those measured using a 2D ^{13}C-{^{13}CO} spin-echo difference CT-HSQC experiment,[8] which relies on detection of the narrow methyl resonance. Together with the small errors in $^3J_{C'C^\beta}$, which are measured from the same spectrum, this indicates that the experimental error in $^3J_{C'C^\gamma}$ is very small (<0.2 Hz). Deriving a Karplus equation for this coupling, however, is less straightforward than for couplings related to the backbone angle ϕ. First, agreement between side chain χ_1 angles in crystal structures of a given protein solved by different groups tends to be far worse than the agreement between backbone angles, which suggests that there is considerable uncertainty in crystal structure χ_1 angles. Second, for many surface residues there is substantial averaging over different rotameric states, and identification of these residues is not straightforward. In addition, for residues not subject to rotamer averaging, there can be substantial differences in the amplitudes of the χ_1 torsion angle fluctuations around a given rotameric state.

On the basis of previous measurements of $^3J_{H^\alpha H^\beta}$, $^3J_{NH^\beta}$, $^3J_{C'H^\beta}$, and $^3J_{NC^\gamma}$ in ubiquitin, in combination with tight distance constraints from ROEs, a subset of 28 ubiquitin residues has been identified for which there is no evidence of multiple rotameric states and which exhibit reasonable agreement between the crystal structure and the above-listed NMR parameters (J. Marquardt and A. C. LiWang, unpublished results). These 28 residues exclude aromatic and Asn and Asp residues, for which $^3J_{C'C^\gamma}$ were reported previously and which have considerably larger *trans* $^3J_{C'C^\gamma}$ values than other residues with less electronegative C^γ substituents. Figure 5 shows the correlation between $^3J_{C'C^\gamma}$ and the $C'-C^\alpha-C^\beta-C^\gamma$ dihedral angle, θ. Clearly, dihedral angles cluster around 180°, corresponding to the most populated $\chi_1 = -60°$ rotamer. However, even for these *trans* couplings, there is a considerable spread in the $^3J_{C'C^\gamma}$ couplings, which range from 2.2 to 4 Hz. Considering that the error in the measurement is the same as for the measurement of $^3J_{C'C^\beta}$, the wide range of *trans* $^3J_{C'C^\gamma}$ values does not result from random measurement error. The possibility that this wide range is related to the C^γ substituents, and thereby would differ by amino acid type, is unlikely for two reasons: First, on the basis of the data shown in Figure 3, $^3J_{C'C^\beta}$ couplings do not exhibit such a dependence on the C^β substituents, and there is no obvious reason why $^3J_{C'C^\gamma}$ would be more sensitive to substituent effects. Second, a wide range of $^3J_{C'C^\gamma}$ values is observed for a given amino acid type. For example, Lys[29] and Lys[48] have $^3J_{C'C^\gamma}$ values of 4.0 and 2.5 Hz, respectively, but according to the crystal structure both have χ_1

(37) Scheiner, S., Kern, C. W. *J. Am. Chem. Soc.* **1977**, *99*, 7042−7050.
(38) MacArthur, M. W., Thornton, J. M. *J. Mol. Biol.* **1996**, 264, 1180−1195.
(39) Tjandra, N.; Grzesiek, S.; Bax, A. *J. Am. Chem. Soc.* **1996**, *118*, 6264−6272.
(40) Karplus, P. A. *Protein Sci.* **1996**, *5*, 1406−1420.

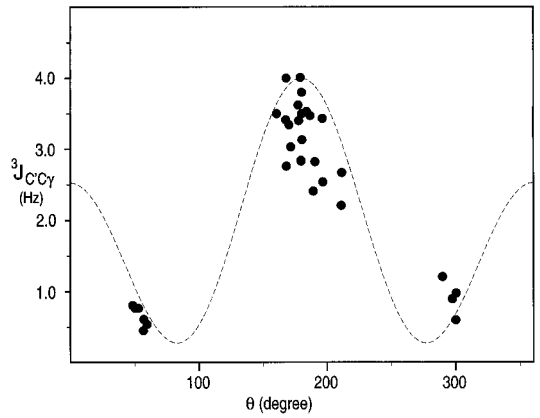

Figure 5. Relation between $^3J_{C'C^\gamma}$ and the corresponding dihedral angle θ ($\theta = \chi_1 - 120°$ for $C^\gamma = C^{\gamma 1}$; $\theta = \chi_1$ for $C^\gamma = C^{\gamma 2}$ of Val; $\theta = \chi_1 + 120°$ for $C^{\gamma 2}$ of Thr and Ile). Only residues for which there is no evidence of χ_1 rotamer averaging on the basis of $^3J_{H^\alpha H^\beta}$, $^3J_{NH^\beta}$, and $^3J_{C'H^\beta}$ values and $d_{N^\beta}(i, i)$ and $d_{N^\beta}(i, i+1)$ ROEs, and for which these parameters indicate a similar χ_1 value in solution and in the crystalline state (J. Marquardt and A. C. LiWang, unpublished results), have been included in this plot.

angles of $-61°$. The possibility that the crystallographically determined χ_1 angle differs dramatically from the one prevalent in solution, or that a significant population of different rotamers are present, have been excluded on the basis of other *J* couplings and ROE data (not shown). Another possibility is that there is a wide range of side chain dynamics, with some residues exhibiting only small χ_1 angle fluctuations and others much larger ones. Without a quantitative assessment of these effects available, it is presently not possible to derive an accurate Karplus curve parametrization for $^3J_{C'C^\gamma}$. However, the maximum value of *ca.* 4 Hz must correspond to a *trans* coupling, whereas the smallest values measured are *ca.* 0.5 Hz, corresponding to dihedral angles in the $60-90°$ range. In contrast, a best fit between the data points shown in Figure 5 and a Karplus curve yields a *trans* coupling of only 3.3 Hz.

The $^3J_{C'C^\gamma}$ couplings are particularly useful for residues where the two C^β methylene protons have identical chemical shifts, as in this case NOE data and $^3J_{NH^\beta}$, $^3J_{C'H^\beta}$, and $^3J_{H^\alpha H^\beta}$ couplings do not yield unambiguous χ_1 angle information. For ubiquitin, Glu^{24}, Gln^{41}, Lys^{48}, Gln^{49}, and Lys^{67} all have degenerate H^β chemical shifts. The respective $^3J_{C'C^\gamma}$ couplings for these residues are 1.5, 3.5, 2.5, 1.5, and 3.4 Hz. Thus, the couplings for Gln^{41} and Leu^{67} indicate *trans* conformations ($\chi_1 \approx -60°$) whereas the χ_1 angles of Glu^{24}, Gln^{49}, and possibly Lys^{48} are either subject to rotamer averaging or deviate strongly from the ideal rotameric states.

Residues 5−9 of apoCaM all show intense correlations in the HN(CO)C spectrum (Figure 2B), corresponding to $^3J_{C'C^{\gamma 1}}$ couplings of 2.7−4.0 Hz and indicative of $\chi_1 = -60°$ rotamers. This agrees with the previously reported solution structure.[32] A total of 74 $^3J_{C'C^\gamma}$ couplings could be identified in apoCaM on the basis of cross-peaks to aliphatic C^γ carbons. For an additional 13 cases, the absence of a C^γ resonance in the HN(CO)C spectrum yields an upper limit of *ca.* 1.5 Hz for $^3J_{C'C^\gamma}$, excluding the possibility of a *trans* conformation.

Concluding Remarks

The sign of long-range $^{13}C-^{13}C$ *J* couplings is not determined by the quantitative *J*-correlation methods. However, it is well established that *trans* couplings are positive. The continuous nature of the observed $^3J_{C'C^\beta}$ couplings as a function of ϕ (Figure 3) indicates that all $^3J_{C'C^\beta}$ couplings have the same sign, i.e., positive. For $^3J_{C'C^\gamma}$ the relation between its magnitude and χ_1 is less well determined. However, considering that only very few $^3J_{C'C^\gamma}$ values in ubiquitin do not give rise to an observable cross-peak, it appears likely all measured $^3J_{C'C^\gamma}$ are positive.

Besides three-bond $^{13}C-^{13}C$ couplings, the method presented here also yields values for the two-bond couplings, $^2J_{C'C^\beta}$ (0.4−2 Hz) and $^2J_{C'C^\alpha}$ (0.4−1 Hz), in both cases with the sign undetermined (Supporting Information). These two-bond couplings also relate to structure. For example, $^2J_{C'C^\alpha} \leq 1$ Hz is indicative of *trans* peptide bonds[33] and, in case C^β carries an electronegative substituent, X, $^2J_{C'C^\beta}$ is related to the $C'-C^\alpha-C^\beta-X$ dihedral angle.[41] However, quantitative interpretation of these two-bond couplings has not been attempted in this study.

Accurate measurement of $^3J_{C'C^\beta}$ and $^3J_{C'C^\gamma}$ is feasible in proteins uniformly enriched in ^{13}C and ^{15}N. Results for the small and rapidly tumbling protein ubiquitin ($\tau_c = 4.1$ ns) indicate that *J* values as small as 0.5 Hz can be measured reliably, with a precision of better than 0.2 Hz. For apoCaM ($\tau_c \approx 8$ ns), the smallest couplings that can be measured are *ca.* 1 Hz and the precision is estimated to be *ca.* 0.4 Hz.

The $^3J_{C'C^\beta}$ values measured for ubiquitin are in better agreement with values predicted by the ϕ angle derived from the other five couplings describing this angle ($^3J_{HNH^\alpha}$, $^3J_{HNC^\beta}$, $^3J_{HNC'}$, $^3J_{C'C'}$, and $^3J_{H^\alpha C'}$) than with the crystal structure ϕ angle. Similarly, $^3J_{HNH^\alpha}$ values predicted on the basis of ϕ angles derived from $^3J_{HNC^\beta}$, $^3J_{HNC'}$, $^3J_{C'C'}$, $^3J_{C'C^\beta}$, and $^3J_{H^\alpha C'}$ agree nearly 2-fold better with experimental results than values predicted on the basis of crystallographic ϕ angles. This indicates that the ϕ angles derived from *J* couplings are highly accurate and self-consistent.

The good agreement between ϕ angles derived from ^3J couplings involving H^N (using the assumption that H^N lies in the $C'_{i-1}-N_i-C^\alpha_i$ plane) with those derived from ^3J values involving C′ confirms that the rms angle between the $H^N_i-N_i-C^\alpha_i$ plane and the $C'_{i-1}-N_i-C^\alpha_i$ plane is smaller than ∼5°. In contrast to previous conclusions, based on agreement between calculated and observed $^{13}C'$ chemical shifts, our data indicate no statistically significant correlation between peptide bond planarity and secondary structure and rule out the presence of substantial pyramidalization at the peptide nitrogen. For α-helical residues in ubiquitin, the average deviation from 180° between the $H^N_i-N_i-C^\alpha_i-H^\alpha_i$ and $C'_{i-1}-N_i-C^\alpha_i-H^\alpha_i$ dihedral angles equals $0 \pm 8°$ ($N = 8$) whereas for β-sheet residues we find $1 \pm 7°$ ($N = 21$).

Measurement of $^3J_{C'C^\gamma}$ is also readily feasible. In contrast to most other NMR methods for determining χ_1, measurement of $^3J_{C'C^\gamma}$ is not hampered by accidental chemical shift degeneracy of H^β methylene protons. The largest $^3J_{C'C^\gamma}$ values (*ca.* 4 Hz) are obtained for the common situation where C′ is *trans* with respect to C^γ (corresponding to $\chi_1 = -60°$, for most types of amino acids). A surprisingly wide range of *trans* $^3J_{C'C^\gamma}$ couplings (2.2−4.0 Hz) is measured, however, even for residues where a significant population of *gauche* rotameric states can be excluded on the basis of other *J* coupling and ROE information. It is likely that this wide range of *trans* couplings results from two effects: a large degree of variation in the amplitudes of χ_1 angle fluctuations and the presence of twisted χ_1 rotamers. Quantitative measurement of side chain dynamics is presently in progress to probe the individual ranges of χ_1 angle fluctuations in ubiquitin.

Acknowledgment. We thank Frank Delaglio and Dan Garrett for software, Andy Wang, Stephan Grzesiek, John

(41) Barfield, M.; Walter, S. R. *J. Am. Chem. Soc.* **1983**, *105*, 4191−4195.

(42) Taylor, J. R. *An Introduction to Error Analysis. The Study of Uncertainties in Physical Measurements*; University Science Books: Mill Valley, CA, 1982.

Marquardt, Nico Tjandra, and Hitoshi Kuboniwa for sharing data on ubiquitin and apoCaM, Janet Thornton for a preprint of ref 38, and David Case, Michael Barfield, Art Edison, and Rod Wasylishen for stimulating discussions. This work was supported by the AIDS Targeted Anti-Viral Program of the Office of the Director of the National Institutes of Health. J.-S.H. is supported by a postdoctoral fellowship from the Cancer Research Institute, New York.

Supporting Information Available: One table containing the $^3J_{C'C^\beta}$ and $^3J_{C'C^\gamma}$ coupling constants measured for human ubiquitin together with the backbone ϕ angles and side chain χ_1 angles derived from the X-ray structure; one table containing the $^3J_{C'C^\beta}$ and $^3J_{C'C^\gamma}$ coupling constants for apoCaM; one table containing the $^2J_{C'C^\alpha}$ and $^2J_{C'C^\beta}$ coupling constants measured for human ubiquitin; one table listing the ϕ and ψ angles derived from the crystal structure, the ϕ angle derived using ^3J couplings involving H^N ($\phi(H^N)$) (assuming planar peptide bond geometry), and the ϕ angle derived using ^3J couplings involving C′ (ϕ-(C′)); one figure showing $\phi(H^N) - \phi(C')$ as a function of the crystal structure ϕ and ψ angles; and two figures showing the rmsd between experimental $^3J_{C'C^\beta}$ or $^3J_{C'C'}$ couplings and those predicted by the crystal structure, when using phase-shifted Karplus equations, as a function of this phase shift (15 pages). See any current masthead page for ordering and Internet access instructions.

JA970067V